Regulation of spike timing in visual cortical circuits

Paul Tiesinga, Jean-Marc Fellous‡ and Terrence J. Sejnowski§||*

Abstract | A train of action potentials (a spike train) can carry information in both the average firing rate and the pattern of spikes in the train. But can such a spike-pattern code be supported by cortical circuits? Neurons *in vitro* produce a spike pattern in response to the injection of a fluctuating current. However, cortical neurons *in vivo* are modulated by local oscillatory neuronal activity and by top-down inputs. In a cortical circuit, precise spike patterns thus reflect the interaction between internally generated activity and sensory information encoded by input spike trains. We review the evidence for precise and reliable spike timing in the cortex and discuss its computational role.

Spike time
The time of occurrence of an action potential, relative to stimulus onset or another event.

Spike volleys
A set of spikes emitted at approximately the same time (typically with a temporal spread of between 1 and 10 ms) by a pool of neurons.

**Physics and Astronomy Department, University of North Carolina at Chapel Hill, North Carolina 27599-3255, USA. ‡Psychology and Applied Mathematics Departments, University of Arizona at Tucson, Arizona 85721-0068, USA. §Computational Neurobiology Laboratory and Howard Hughes Medical Institute at the Salk Institute, La Jolla, California 92037, USA. ||Division of Biological Sciences, University of California at San Diego, La Jolla, California, 92039-0348 USA.*
e-mails: tiesinga@physics.unc.edu; fellows@email.arizona.edu; terry@salk.edu
doi:10.1038/nrn2315
Published online
17 January 2008

Reliability and precision are two different quantities. When you make an appointment with your friend, she can either keep the appointment or not show up at all. If she does show up, she might or might not be on time. The former uncertainty is related to reliability, whereas the latter is related to precision. When the same stimulus waveform is repeatedly injected at the soma of a neuron *in vitro* (FIG. 1a), a similar spike train is obtained on each trial[1,2] (FIG. 1b). When approximately the same number of spikes occur on each trial the neuron is said to be reliable, whereas when the spikes occur almost at the same time across trials it is said to be precise (FIG. 1c). For a single neuron, the potential information content of precise and reliable spike times is many times larger than that which is contained in the firing rate, which is averaged across a typical interval of a hundred milliseconds[3–6]. The information contained in spike timing is available immediately, rather than after an averaging period. Furthermore, the timing of patterns of spikes can potentially transmit even more information than the timing of the individual constituent spikes[3,7]. The potential relevance of spike patterns becomes apparent when we consider neurons at the population level: when a group of similar neurons (a 'pool') produces precise and reliable spike trains, the neurons they project to receive volleys of synchronous spikes[8,9]. This opens up the possibility of communicating between different cortical areas through synchronous spike volleys.

In contrast to the *in vitro* situation described above, in the intact cortex most excitatory synaptic inputs arrive at the dendrites rather than at the soma (FIG. 1d), and synaptic transmission is typically unreliable[10–13]. Furthermore, most of these dendritic inputs are not directly related to ongoing sensory stimulation; rather, they reflect spatiotemporally structured internal activity. Therefore, when the same stimulus is presented repeatedly, the resulting spike trains are usually neither precise nor reliable when they are aligned to the stimulus onset[6]. Instead, neural activity *in vivo* might be dominated by internally generated complex reverberations or rhythmic oscillations, and precise and reliable spike trains might only emerge after they have been aligned according to the phase of the oscillation (FIG. 1e).

Current technologies are progressing to the point where it is possible to record the simultaneous spiking activity of hundreds of neurons, as well as to manipulate their spike timing[14,15]. However, without a theoretical framework for understanding cortical information processing, such data might not be easily interpretable. A key to cortical computations is the integration of feedforward and top-down information, which occurs at the level of the single cortical neuron. In order to fully understand this process we need to determine the computational role of precise and reliable spike times. This Review focuses on precisely emitted spike patterns and their theoretical implications, and aims to set the stage for the large-scale study of cortical information processing. We review the biophysical mechanisms that are responsible for generating spike patterns and describe methods for uncovering spike patterns in the presence of cortical background activity. Finally, we link the integration of temporally precise synaptic inputs in active dendrites to communication, using spike volleys, within and between cortical areas.

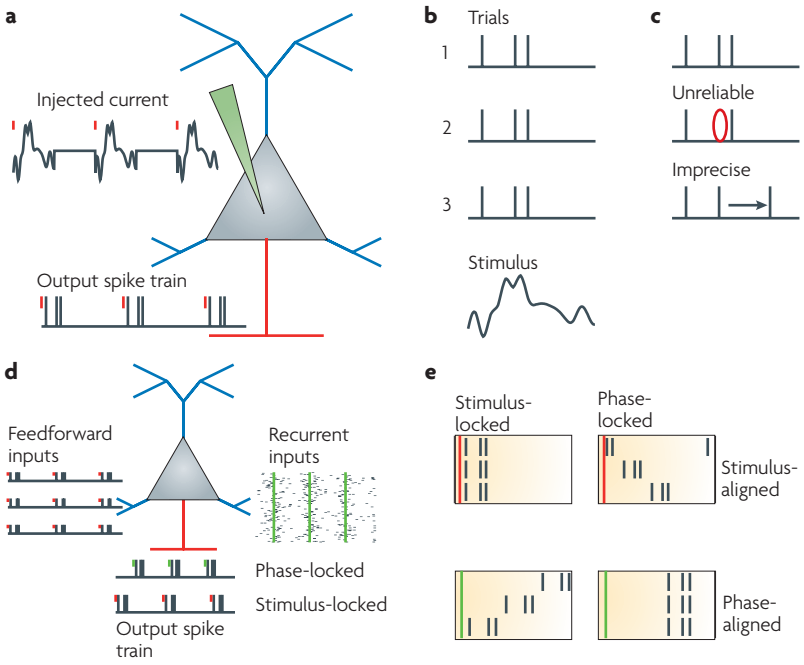

Figure 1 | **Stimulus locking *in vitro* and *in vivo*. a** | An *in vitro* reliability paradigm. A current consisting of many repeats of a short stimulus waveform followed by a period of zero current is injected using an electrode at the soma. The start of the stimulus is indicated by a red dash. The corresponding output spike train is shown at the bottom. **b** | Trials are aligned with the red dashes (the stimulus waveform is shown at the bottom). When the neuron is stimulus-locked, the spike trains are similar across trials. **c** | When spikes are missing in some trials but not in others, the neuron is considered unreliable. When the spike occurs but the spike time is variable, the neuron is considered imprecise (BOX 1). **d** | *In vivo*, the neuron receives feedforward inputs and recurrent inputs. When the same stimulus is presented repeatedly (represented by the red dashes), presynaptic neurons produce spike trains with repeatable motifs — spike patterns — that are similar in each neuron. Across a population, this input consists of a sequence of synchronized spike volleys. Recurrent inputs are periodic when the neuron is embedded in an oscillatory network. The beginning of each oscillation cycle is indicated by the green dashes. Two types of output spike train are shown: a stimulus-locked train and a phase-locked train. **e** | When the neuron is stimulus-locked, precise and reliable spike trains are obtained only when the trials are aligned with stimulus onset. When the neuron is phase-locked, precise and reliable spike trains emerge only when the spike trains are aligned with the start of the oscillation cycle.

What can we learn from spike patterns *in vitro*?

Precision and reliability of* in vitro *spike trains. When a cortical neuron in a slice preparation is repeatedly injected with the same current waveform it produces precise and reliable spike trains[1]. A spike-time histogram generated from the results of multiple trials of either *in vitro* or model neurons shows transient peaks corresponding to spike alignments, which are referred to as events (FIG. 2a–c). Quantitatively, the reliability of an event is the fraction of trials on which a spike occurs at that time[1,16]. The response is said to be precise when the standard deviation of the spike times (also referred to as the 'jitter') in an event across trials is small. In principle precision and reliability are independent quantities, but in practice they are often related[17]. For most experimental data sets it is not straightforward to calculate the precision and reliability because of background noise. There are several different ways to obtain these measurements (BOX 1).

***Detecting spike patterns* in vitro.** A single-neuron spike pattern is a sequence of spike times that either occur together in a trial or do not occur at all. For example, a neuron can respond to a certain segment of a stimulus with a pattern comprised of two spikes that are always separated by 18 ms. Analysis of data recorded from a motion-sensitive neuron in the fly brain shows that such spike pairs provide more than twice the information provided by single spikes[7], suggesting that information is coded in the pattern in addition to in the individual spike times. A first step in evaluating the possible role of spike patterns in cortical slices *in vitro* is to detect them. For a series of trials, the data can be arranged to form a similarity matrix, and a clustering algorithm can be used to identify spike patterns. Spike patterns have been uncovered in experimental data using this procedure[18], which is illustrated in FIG. 3 for data taken from a model neuron.

Factors affecting reliability and precision. Simple models of an *in vitro* preparation in which synaptic transmission is blocked and the same somatic current is injected repeatedly suggest that imprecision is mainly due to variability in the membrane voltage just before the spike, and that this is inversely proportional to the rate of change of the voltage[19,20]. Thus, a precisely timed spike follows a rapidly depolarizing current. There are other sources of imprecision: the spike threshold can change with the rate of voltage change[21] or membrane currents can be activated by neuromodulators. As the rate of change of the membrane voltage generally increases with the amplitude of the stimulus, the precision should improve as the stimulus amplitude increases; this has indeed been observed both *in vitro*[22,23] and *in vivo*[24,25].

In the situation described above, trial-to-trial unreliability results from a failure of spiking, which occurs when the membrane voltage does not reach the spike threshold. In this circumstance, the maximum voltage deflection caused by the stimulus is, on average, below the threshold. The probability of spike failure then depends on how far the peak is below the threshold and on how broad the peak is. The following argument shows that spike failure can lead to distinct spike patterns. For the model neuron described above and in FIG. 3, spikes occur at or close to peaks in the stimulus waveform. When, on a given trial, a peak is missed, the neuron might spike at the next available peak. On a trial in which the neuron does spike on the first peak, it might not be able to spike on the next peak because of afterhyperpolarization currents or other intracellular events. On these two trials the neuron's spikes will correspond to two distinct sequences of peaks (FIG. 3g). Across the two trials the neuron will thus produce distinct spike patterns[18,26], as observed *in vitro*[19,23]. When there is a prolonged period without spiking on both trials, the voltage trajectories will converge back and the same spike pattern will be obtained.

Stimulus locking and phase locking. Precision in spike timing depends on a neuron's firing being locked to features of the stimulus, meaning that whenever a feature appears in the stimulus a spike will be produced with a

Feedforward information
In the context of stimulus–response circuitry, feedforward information is information that is processed in a single direction — from sensory input through perceptual analysis to motor output — without involving feedback information flowing backwards from 'higher' centres to 'lower' centres.

Top-down information
The flow of information from 'higher' to 'lower' centres, conveying knowledge derived from previous experience rather than from sensory stimulation.

constant delay[27]. For a constant-current pulse, the only feature that a neuron can lock on to is the onset (illustrated for a model neuron in FIG. 4a). For an aperiodic or periodic drive, a spike is more likely to occur during certain time intervals (those in which there is a brief depolarization) than during others (those in which there are brief hyperpolarizations) (FIG. 4b,d). This phenomenon is referred to as stimulus locking (or phase locking when the drive is periodic)[1,2]. An *in vitro* study demonstrated that the strength of stimulus locking could, in principle, be increased in feedforward networks[8]. When a pool of similarly responding neurons generates a moderately precise volley as input to the next pool, the volley produced by the latter pool will be more precise. However, this study assumed that synaptic transmission from one pool to the next was perfect, and probably overestimated the amount of reliability and precision that would be present in feedforward networks *in vivo*.

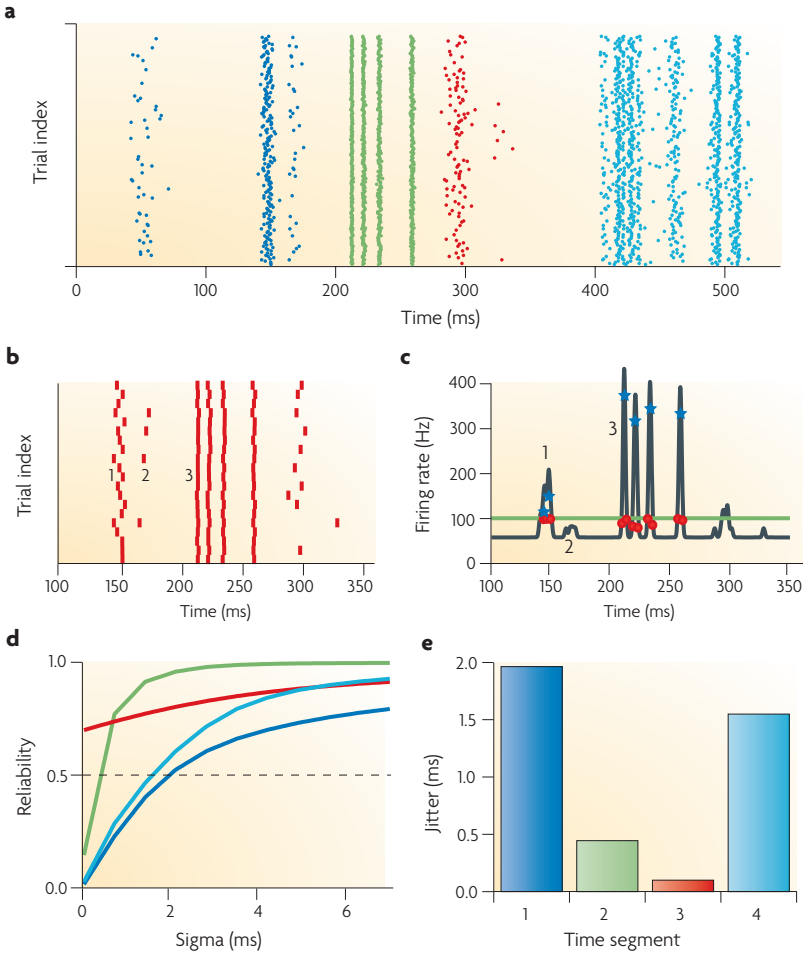

Figure 2 | **Calculating the reliability and precision of neural spike trains.** **a** | The spike trains shown were obtained from simulations of a model neuron with Hodgkin–Huxley-type voltage-gated channels driven by a fluctuating current[26]. Similar trains could be obtained experimentally from neurons *in vitro*. The rastergram shown was constructed by plotting the spike train for each trial on a separate row, aligned with stimulus onset. The y ordinate of each tick is the trial number and the x ordinate is the spike time relative to the stimulus onset. For further analysis the data were divided into segments (shown in different colours). **b** | Twenty trials from part **a** from the time interval between 100 and 350 ms relative to the stimulus onset, showing that precision and reliability are distinct quantities. Event 1 is reliable — that is, a spike occurs on each trial — but it is not precise (there is a large jitter). Event 2 is precise but not reliable. Event 3 is both precise and reliable. **c** | Spike-time histogram, showing how the average firing rate (the number of spikes per second) across a series of trials changes with time. Events (blue stars) are peaks in the histogram and event reliability is the area under the peak. A threshold (the green line) is set, to define the events. When the threshold is set too high, unreliable events (such as event 2) are missed; when it is set too low, noise spikes could be interpreted as events. For the purpose of the reliability calculation (described in a previous publication; see REF. 135), each spike is replaced by a waveform of width sigma. The parameter sigma represents the temporal resolution of the spike times. **d** | Reliability as a function of sigma. Each curve is colour-coded to match the colour of the time segment in the rastergram (**a**) that was used in the calculation. The jitter (the standard deviation of the spike times in an event) corresponds approximately to the value of sigma for which the reliability becomes more than 0.5. The precision is equal to 1 divided by the jitter. **e** | The jitter for each segment. The third segment (shown in red) never intersects 0.5 and the jitter is not defined.

Many neurons have a preferred frequency for stimulus waveforms, which affects the type of oscillation to which they can phase-lock. For a subthreshold sinusoidal current, the amplitude of the voltage deflection will be maximal when the stimulus frequency matches the preferred frequency. This can be demonstrated *in vitro* by injecting a sinusoidal current with a frequency that changes slowly across time. The neuron's membrane-voltage oscillations will match the instantaneous frequency of the drive, but the amplitude of the oscillations will vary, reaching a maximum when the instantaneous frequency matches the preferred frequency[23,28,29]. When the stimulus amplitude is increased above the spike threshold, the firing rate, reliability and precision will be optimal for stimulus waveforms at the neuron's preferred frequency. Experiments show that preferred frequencies depend on neuron types[23,30,31]. Models predict that the preferred frequency arises from the dynamics of voltage-gated channels[32–34].

When a neuron is injected with a constant current, after a period of adaptation it will produce an approximately periodic spike train. The frequency of the spike train will be equal to the average firing rate of the neuron (the direct current (DC) firing rate), which depends on the amplitude of the current, but this spike train will not be precise across trials[1] (model results are shown in FIG. 4a). When a small periodic drive is added (FIG. 4b), however, the precision will improve significantly when the stimulus frequency matches the DC firing rate[19,35,36]. This phenomenon occurs even when the neuron does not have a subthreshold preferred frequency. Neuromodulators generally have multiple effects in cortical circuits. For instance, they can change the DC firing rate of the neuron[37,38]; this particular effect can be modelled as an additional depolarizing or hyperpolarizing current. Hence, in the model described above, neuromodulators can in principle alter the DC firing rate so that it approximately matches the oscillation frequency of the network that the neuron is embedded in. This not only improves the precision of the neuron by way of phase locking[32] but also increases the postsynaptic impact of a pool of such neurons[26]. For instance, in a model of odour recognition[39], a group of neurons driven at the same firing rate achieved spike synchronization by phase locking to a common oscillation.

Spike-time histogram
A tool for resolving the behaviour of the firing rate as a function of time, by averaging across multiple trials or multiple neurons. Mathematically, it is obtained by counting the number of spikes in each time bin and normalizing the count by the bin width, the number of trials and/or the number of neurons.

Event
A time-point relative to the stimulus onset during which a spike is found on a significant fraction of the trials.

What do we know about spike patterns *in vivo*?

Although spike patterns have been found *in vitro* in response to current injection at the soma, they can only have a role in information processing if they are also present *in vivo*. Here we review the evidence for spike patterns *in vivo*, using the visual system as our focus, and discuss the influence of receiving temporally coherent synaptic inputs due to oscillations. Finally, we discuss how the spike timing of a neuron is affected by dendritic synaptic inputs.

Evidence for spike-time precision in the visual system. Precise spike firing has been found at almost all levels of the mammalian visual pathway. In an eye-cup preparation, retinal ganglion cells produced precise and reliable spike trains in response to a temporally fluctuating visual stimulus[24,25,40–42]. Precision increased as stimulus contrast increased, because of an enlargement in the somatic amplitude of the inputs. Neurons in the lateral geniculate nucleus, which are driven by retinal ganglion cells, have been shown to respond precisely and reliably to a sequence of spatially uniform image frames with a fluctuating luminance[3,43]. When recordings from cells of the same type in different animals were compared, most of the events occurred at similar times during the stimulus presentation[43]. It is likely, therefore, that in the same animal multiple neurons produce spikes at similar times, resulting in synchronous volleys to the primary visual cortex[44].

Neurons in layer 4 of the primary visual cortex can also fire with high precision in response to visual inputs[45,46]. Neurons in the mediotemporal cortex in turn receive inputs from the primary visual cortex and respond to motion. It has been shown that neurons in the mediotemporal cortex respond precisely to rapid changes in the direction of motion[47]. The reliability of events in these spike trains was initially found to be low; however, a re-analysis revealed multiple reliable spike-time patterns[18]. Further evidence for precise spike timing at this level is found in the barrel cortex[48] and the auditory cortex[49].

Overall, the degree of precision of spiking in response to repeated presentations of the same stimulus appears to decrease along the visual pathway[50], whereas spike-count variability increases[42,43,47,51–53]. This could be due to the presence of background cortical activity, in which case a method to uncover the stimulus-locked precision is needed (FIG. 1d).

The contribution of cortical oscillations to precision. In addition to stimulus-related feedforward inputs, neurons *in vivo* are driven by internally generated network activity. Electroencephalograms (EEGs) recorded from the human scalp exhibit superposed rhythms in various frequency ranges, including the delta (0.5–4 Hz), theta (4–8 Hz), alpha (8–12 Hz), beta (12–30 Hz) and gamma (30–80 Hz) ranges[54]. The strength of these rhythms changes over time and depends on behavioural states and cognitive processes[55–57]. The rhythms arise from large-scale, coherent firing of neurons. Extracellular recordings of local field potentials (LFPs) directly from the cortex reveal bursts of oscillatory activity. These might modulate stimulus-related activity, either directly (by providing additional synaptic inputs) or indirectly (by generating gradients in the extracellular potential[58]), and thus might cause the apparent imprecision of cortical responses described above.

The frequency, amplitude and phase of these cortical oscillations are modulated by cholinergic and GABAergic subcortical projections from the basal forebrain and from other diffuse neuromodulatory systems[59,60]. A visual stimulus can reset the phase of an ongoing alpha rhythm[61], and cortical connections can also modify the phase of ongoing oscillations[62,63]. Thus, the phase and amplitude of cortical oscillations can be modulated to alter the precision and timing of spike volleys. Measurements *in vivo* could detect this as a modulation of both the precision of the phase-locked responses and the spike phase relative to the oscillation.

***Evidence for phase locking* in vivo.** A fundamental challenge in neuroscience is to characterize the relationship between the input to a cortical area and the resulting output spike trains that are transmitted to other cortical areas. The relationship between the LFP and the

Box 1 | Methods for determining the precision and reliability of spike trains

The direct method

In the direct method for determining spike train precision and reliablity, a spike-time histogram is constructed, as described in FIG. 2. Spike alignments are classified as events when the histogram exceeds a threshold (FIG. 2c): all spikes are either assigned to an event or classified as background. Event reliability is calculated directly and event precision is the inverse of the standard deviation of all the spike times assigned to an event. Reliability and precision are the average event reliability and event precision across all events, respectively.

Indirect methods

In the indirect method, statistics related to the reliability of events are calculated based on all spike times without detecting the events themselves. In one method, spike trains are transformed into a continuous waveform for each trial; each spike is convolved with a Gaussian distribution that has a standard deviation sigma[135,136]. The stronger the spike alignment between two trials, the larger the overlap between the two waveforms will be (calculated as the cosine of the angle between the two waveforms when the waveforms are considered as vectors). This quantity is a number between 0 (entirely different spike trains) and 1 (identical spike trains) and is called the similarity (S_{ij}). The reliability estimate, R, is the mean of S_{ij} across all distinct pairs. Intuitively, S_{ij} measures the degree of overlap between spike times on the two trials i and j. Sigma determines which spike times between the pairs are considered overlapping and sets the timescale of the similarity measure. Typically, sigma is taken to be a few milliseconds. In experimental data, the precision of the firing often varies with time. This can be dealt with by segmenting the data into small chunks and determining the R value for each. The precision can be estimated by calculating the reliability as a function of sigma. The inverse of the sigma at which R is 0.5 provides an estimate for the precision (FIG. 2d). Alternative measures to determine the difference between spike trains, such as the Victor–Purpura metric[137] or the van-Rossum metric[138], can be converted to a similarity measure that is suitable for a reliability analysis.

An alternative method

Indirect methods always require a choice of parameter, such as sigma. By contrast, the direct method yields independent estimates for the reliability and precision. An even simpler measure[115] starts with the spike times merged across all trials and arranged with the earliest spike first. The inter-spike intervals of this sequence are then calculated and the coefficient of variation of the aggregate response (CVP) is calculated as the standard deviation of the inter-spike intervals divided by their mean. A similarity measure normalized between 0 (unreliable) and 1 (perfectly reliable) is obtained by subtracting 1 from the CVP and dividing by the square root of the number of trials.

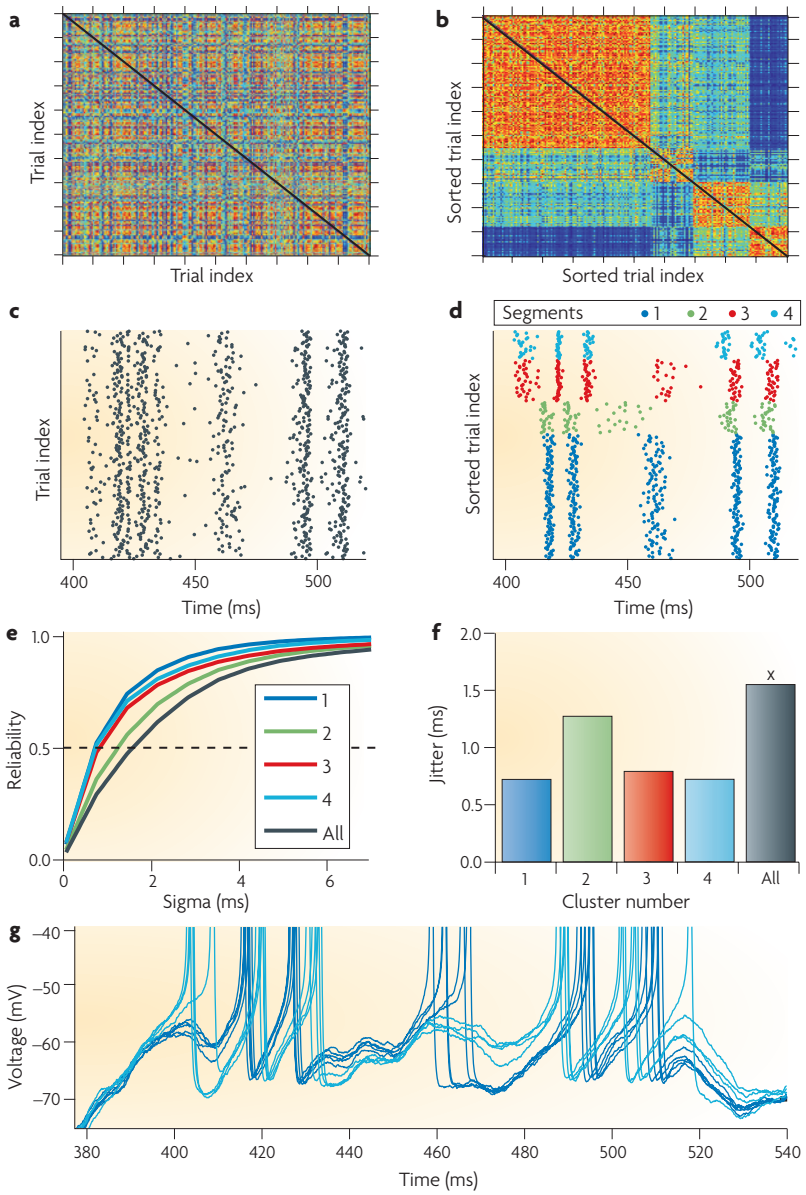

Figure 3 | **Uncovering spike patterns. a**,**b** | Having identified precise and reliable spike trains (see FIG. 2), spike patterns can be revealed. The value of the similarity (S_{ij}) between the spike train on trial i and the spike train on trial j is represented as the colour of the pixel on row i and column j**.** On the colour scale, blue indicates low similarity and red indicates high similarity. **c**,**d** | The rastergrams from which the similarity matrices in **a** and **b**, respectively, were calculated (the data were taken from the fourth segment (shown in cyan) of FIG. 2a). In **a** and **c** the trials are ordered as they are recorded, whereas in **b** and **d** they are reordered using fuzzy K-means clustering[139] to bring similar trials close to each other[18]. Spike patterns are operationally defined as groups of trials that are more similar to each other than to the other trials. In **a** no obvious structure is visible, but in **b** spike patterns have been uncovered. These patterns correspond to square blocks, with high similarity values on the diagonal. In **d** each spike pattern is shown in a different colour. The spike patterns had different spike times and, in some cases, a different number of spikes. **e** | Reliability is the average degree of similarity between pairs of spike trains at the temporal resolution given by the parameter sigma (BOX 1). Reliability is plotted against sigma for each spike pattern. **f** | The jitter (the standard deviation of the spike times in an event) for each spike pattern and across all trials. The precision (the inverse of the jitter) that is evaluated for each pattern separately is much higher than that which is calculated with all trials combined. **g** | Voltage traces corresponding to clusters 1 and 4. Cluster 4 spikes at 405 ms whereas cluster 1 does not; at 460 ms the situation is reversed. After a transient hyperpolarization that prevents spiking, the two voltage traces are close to convergence at 540 ms. This graph shows that spike patterns correspond to distinct voltage trajectories[26].

recorded spike trains is particularly important as the LFP is dominated by subthreshold currents that represent inputs to nearby neurons and as the spikes reflect the output of neurons that project more distantly. Because a periodic drive is generated at the soma during network oscillations, phase-locked responses are expected *in vivo*. In a landmark experiment, researchers recorded from different types of hippocampal interneurons during theta LFP oscillations[64–66] and sharp wave ripples (brief oscillations with frequencies between 80 and 150 Hz)[67]. Different interneuron types locked at specific phases with respect to the LFP, and the phases that they locked to also depended on the frequency of the oscillation. *In vivo* studies have also revealed evidence for phase locking in the neocortex[57]. In cortical area V4, the correlation in the gamma frequency range between spike trains and the LFP near the recorded neuron increased during attention[56,57]. Similarly, in a behavioural task in which a monkey had to hold a stimulus in working memory[68], locking of spikes to the theta oscillation was increased in response to a neuron's preferred stimulus compared with a non-preferred stimulus, independent of changes in the neuron's firing rate. In the human brain, spike trains are also locked to the LFP in specific frequency bands, which depend on the area involved[69]. For example, locking to the gamma band was more prominent in the frontal region of the brain than in the parietal and temporal cortices. Correlations also occur between distant brain areas: the spike trains in rodent prefrontal cortices correlate with the hippocampal LFP, with approximately a 50 ms delay[70]. A procedure to uncover this type of phase-locking is illustrated in FIG. 5.

Phase locking and stimulus locking in the cortex. A cortical neuron receives on the order of 10,000 synaptic inputs[71], most of which are from other cortical neurons and only a small fraction of which are active at any one time. Although a stimulus waveform is locked to the stimulus onset, the phase of oscillations is set internally and is therefore typically not connected to the stimulus onset (however, in a recent *in vivo* experiment, the phase of ongoing delta oscillations became locked to the onset of auditory stimulation, which was presented with an inter-stimulus interval that was comparable to the period of the delta oscillations[63]). The precision of firing therefore reflects a balance between intrinsic reverberations (including oscillations) and stimulus properties[72].

In a cortical model, when spikes are generated in response to stimulus-related inputs independently of those that are generated in response to oscillatory inputs, stimulus-locked and phase-locked responses can be obtained at the same time (FIG. 6a,b). However, in general there will be interaction between these two types of input. Depending on the nature of the interaction, stimulus locking can still be obtained. For instance, stimulus locking persists when the oscillatory inputs change the number of spikes that a neuron produces in response to the stimulus-related inputs, but not their timing (FIG. 6c), or when the shift in spike times caused by the oscillation is small (FIG. 6d). Single-compartment models[73] predict a strong interaction that almost surely will destroy stimulus locking

Neuromodulator
An endogenous chemical substance that changes the intrinsic properties of a neuron and the dynamics and strength of neurotransmission. Neuromodulators can modify neuronal responses to synaptic inputs on potentially long timescales.

Afterhyperpolarization
The membrane hyperpolarization that follows the occurrence of one or several action potentials.

Eye-cup preparation
A preparation in which the retina is extracted intact so that the neural responses to activation of the photoreceptors by a visual stimulus can be recorded.

Local field potential
(LFP). The total electrical current in the vicinity of the recording electrode, reflecting the sum of events in the dendrites of a local neuronal population. It is often obtained by low-pass filtering (that is, removal of signals lower than 600 Hz) of the recorded electrical signal.

Compartmental model
A computer model that breaks a neuron down into small electrical compartments and can simulate the propagation of electrical signals inside the neuron and across its membrane surface.

and phase locking, because the two types of input arrive at the same compartment. However, in compartmental models the interaction is weaker because the synaptic inputs are spatially segregated. Because *in vivo* neural responses can alternate between stimulus-locked epochs and phase-locked epochs[72], averaging to extract either the stimulus-locked or the phase-locked response should be carried out with care.

Propagation of spike patterns in cortical networks

The preceding sections have documented the presence of spike patterns and phase locking at the level of individual cortical neurons. How can these patterns be retained or further processed in cortical circuits?

Synfire chains in cortical networks. Precise spike times can lead to synchronous spike volleys in pools of neurons that can propagate from pool to pool in model[74] and *in vitro*[8] feedforward networks with a precision that depends on a number of physiological parameters. The sequential activation of multiple pools is referred to as a synfire chain (or as 'cortical songs'[75]). Synfire chains have been embedded in large-scale model networks by increasing the number of synaptic connections between selected pools of neurons. In those networks, the synfire mode of propagation was often associated with large-scale wave-like activity propagating through the network, after which the network became refractory[76].

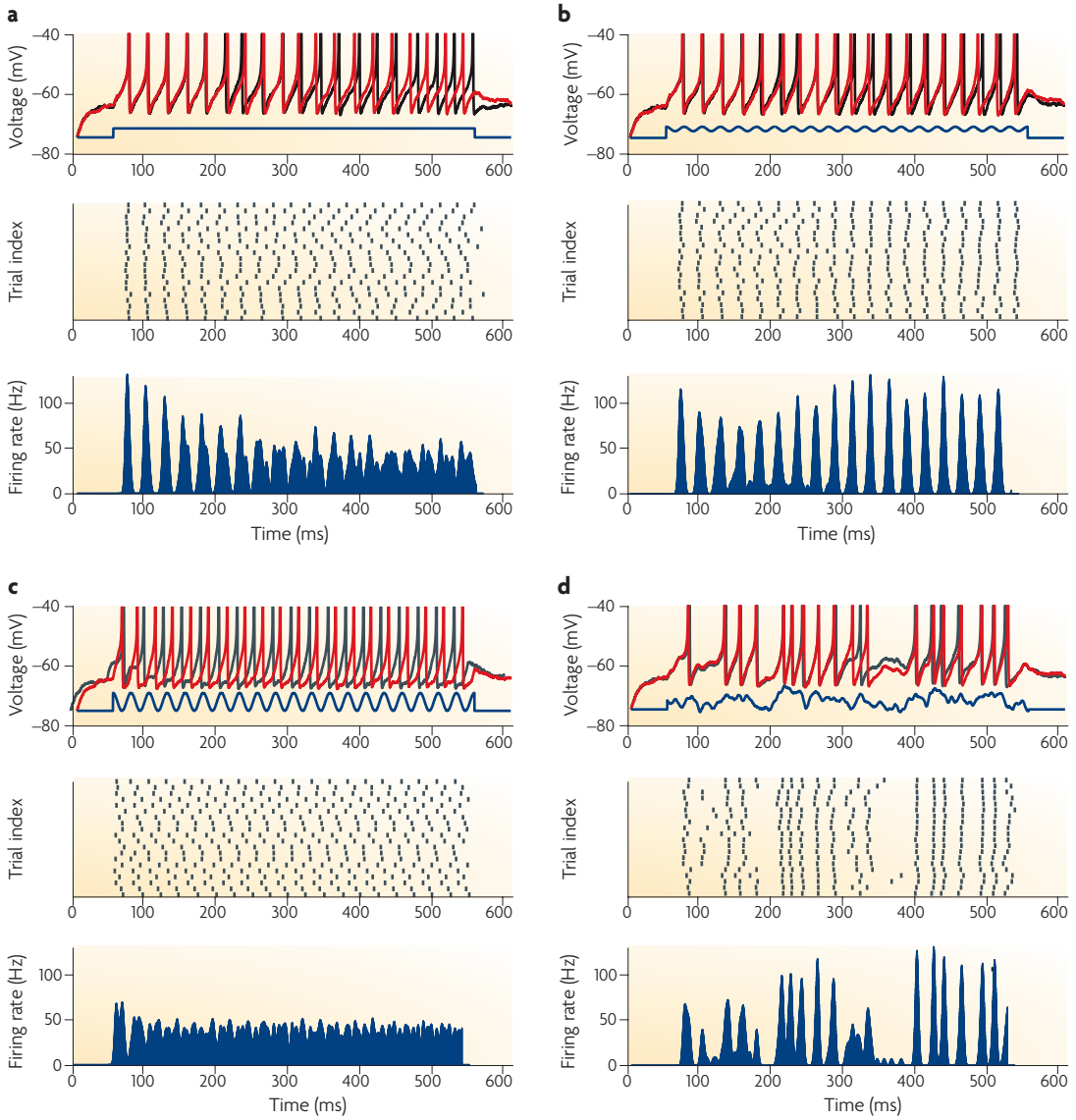

Figure 4 | **The effect of a periodic or an aperiodic drive on reliability in a model neuron.** Each part shows, from top to bottom, a graph with two voltage traces (the red and black lines) and the stimulus waveform (the blue line), a rastergram and a histogram. The model neuron used in FIG. 2 provided the data. **a** | In response to a current step, precision decreases over time. **b** | When a periodic current is superimposed, the precision is maintained because of a resonance effect. The firing rate is approximately the same in **a** and **b**. **c** | When the phase of the periodic drive is varied from trial to trial the precision is reduced (the stimulus waveform is only shown for one phase). **d** | In response to an aperiodic current, well-defined events with a range of precisions are obtained.

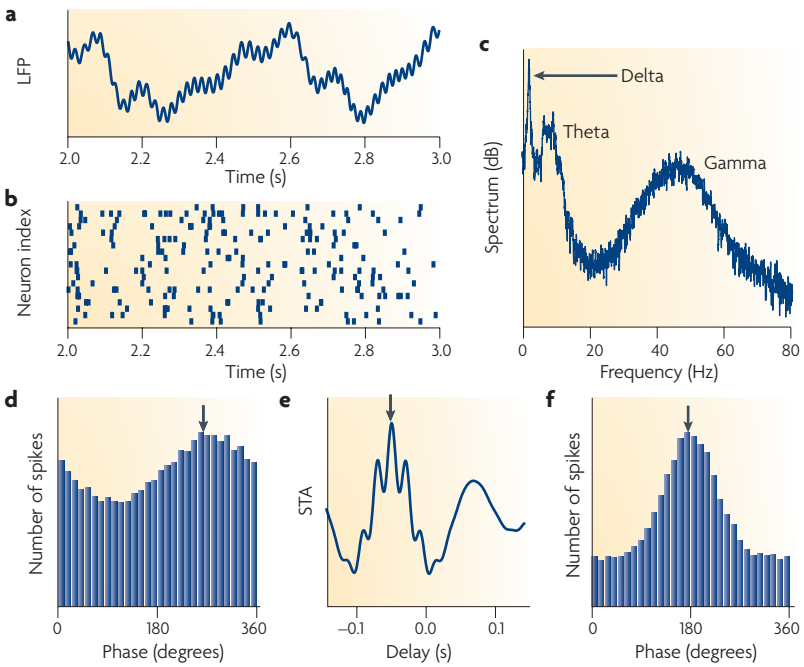

Figure 5 | **Uncovering phase locking to internal activity.** Phase locking to internal activity is uncovered by analysing simultaneously recorded spike trains and the local field potential (LFP) generated by a simple model. **a** | A short segment of an example LFP trace that was constructed by adding three noisy sinusoidal waveforms with frequencies in the gamma, theta and delta frequency ranges. **b** | Sample spike trains were constructed to be weakly phase-locked, in the gamma frequency range and at a delay of 50 ms, to the example LFP. **c** | The three peaks in the power spectrum of the example LFP reveal the presence of the frequency content in gamma, theta and delta. **d** | A histogram of the phase of the gamma oscillation at the spike times shown in part **c**. The peak (indicated by the arrow) shows that the spikes have a weak preference for a phase of 270 degrees, which means that they are weakly phase-locked. The histogram looks smooth because it is averaged across 200 neurons firing at 10 Hz during a 40-second segment. This raises the issue of how to find groups of similarly responding neurons in multi-electrode recordings without knowing their behaviour. The clustering procedure introduced in FIG. 3 is useful in this regard. **e** | The spike-triggered average (STA) of the LFP is obtained by collecting, for each spike, the LFP waveform in the interval from 12.5 ms before to 12.5 ms after the spike. The STA is the average across all collected waveforms. The peak (indicated by the arrow) shows that spikes are most correlated with the LFP 50 ms in the past. **f** | A histogram of the phase of the gamma oscillation 50 ms before the spike times in part **c**. The neuron spikes preferentially at a phase of 180 degrees. The peak is sharper than in part **d**, which means that the true precision of phase locking was uncovered.

Another modelling study[77] determined whether information could reliably propagate from one pool of neurons to another in the presence of internally generated background activity in a random network in which a synaptic connection was made between a small fraction of neuronal pairs. On average, a neuron received synapses from no more than 2% of the neurons in the network. Seven pools that were connected in a feedforward fashion were selected. The intrinsic properties of the neurons were parametrically varied and the connections between neurons in consecutive pools were strengthened (analogous to the effects of spike-timing-dependent plasticity[78]). These studies showed that volleys either died out or propagated between pools, recruiting more spikes at each stage. In the latter case the timing information was lost, because it was not possible to determine when the response to one volley ended and the response to another began. Firing-rate information was transmitted more easily when square pulses of increased external activity were injected into the first pool. Firing rates modulated on a timescale of a few tens of milliseconds could also be transmitted, but some distortions in the shape of the transmitted waveform occurred. Based on a single-compartment model, which assumed that the membrane potential of the entire neuron was uniform, the results suggested that in a sparse randomly connected network it is difficult to obtain robust and reproducible signal transmission along a synfire chain. However, real neurons are spatially extended, so the efficacy of a given synapse might depend on its location and on the concurrent activity of other synapses in a highly nonlinear way (see below). In addition, specific network architectures (that is, ones that are not sparse or random) might facilitate the reproducible propagation of volleys. These two possibilities are reviewed in the following subsections.

Results that are consistent with the existence of synfire chains have been reported in slice experiments that measured calcium transients from many neurons, but direct evidence for synfire chains is still absent. Recordings have revealed repeating patterns of activation arising from a sequence of neurons that became active in the same order[75]. The patterns repeated more often than would be expected from random activation[75,79] (but see REF. 80 for an alternative view). However, the spiking precision is difficult to determine because individual spikes cannot always be resolved.

Decoding synchronous inputs in spatially extended neurons. Cortical pyramidal cells need to integrate information from many sources. For example, a layer 5 pyramidal cell[81,82] has access to inputs from all cortical layers and must integrate these into one single spike train. Historically, dendrites have been modelled as passive structures with a specific resistance and a capacitance[83]. However, studies over the past two decades have demonstrated the non-uniform distribution of many types of voltage-gated channel on dendrites[84]. The functional relevance of these channel distributions is only now starting to emerge[85–87].

For a passive dendrite, the voltage deflections that result from two excitatory inputs can be estimated as the sum of the individual deflections. This is an overestimate, because the depolarization caused by the first input reduces the driving force for the second input. Therefore, when the response actually exceeds the sum of individual responses, additional nonlinear mechanisms must be responsible. For instance, these can be based on the activity of dendritic calcium channels and NMDA (*N*-methyl-D-aspartate) receptors[85]. To estimate the nonlinearity, the voltage deflection at the soma that arises from multiple inputs on the same dendritic branch of a layer 5 pyramidal cell was determined[88]. When the measured response was plotted against the summed response a sigmoidal relationship was found. For weak inputs the relationship was linear[89], but for strong inputs the measured response increased rapidly with input strength and then saturated. When the same experiment

Cortical pyramidal cell
A class of neuron in the cerebral cortex with a pyramid-shaped cell body. These neurons have dendrites that extend locally and can project their axonal processes both locally and distally across many layers and brain areas.

Caged glutamate
An inactive derivative of glutamate that can be transformed into the active transmitter, usually by photolysis. This technique provides an efficient means for achieving a spatially restricted application of glutamate.

Dendritic action potential
(dAP). An action potential that is first generated in the dendrites and which then propagates towards the soma, often but not always eliciting a somatic action potential after a brief delay.

Relay cell
A type of cell in the thalamus that sends its axon to the cortex. Relay cells in the lateral geniculate nucleus receive inputs from the retina and project to spiny stellate cells in layer 4 of the primary visual cortex.

Spiny stellate cells
(SSCs). An excitatory cell type that is common in layer 4 of the sensory cortex. SSCs have axons that have a local arborization pattern and have dendrites that are covered by spines.

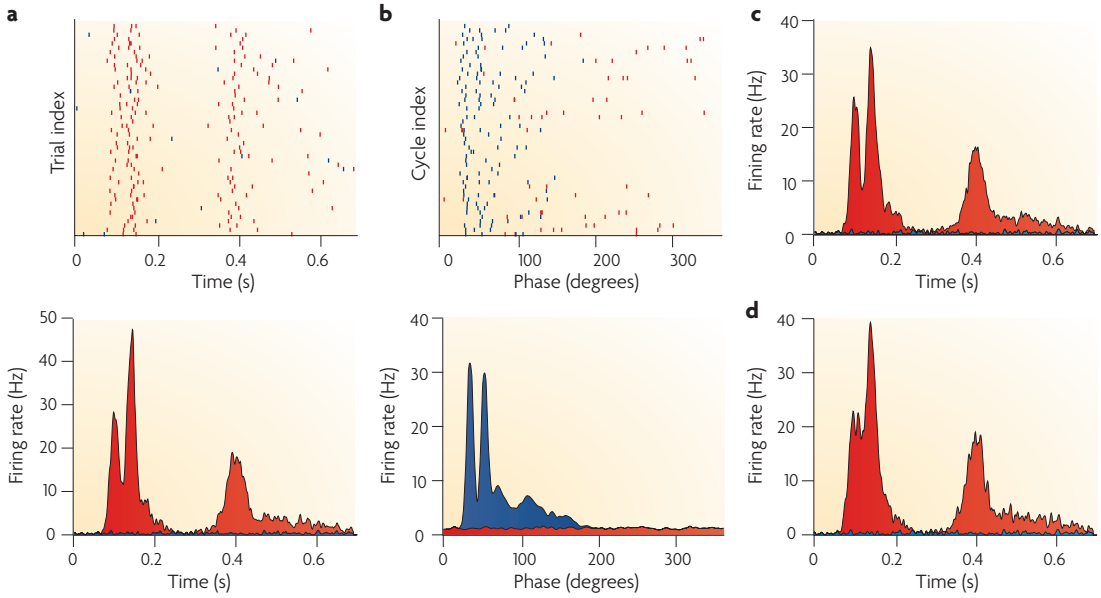

Figure 6 | **Response of a model cortical cell to stimulus-related and oscillatory background synaptic inputs.** A model cell was embedded in a network producing a delta oscillation. A stimulus lasting 0.7 seconds was presented 1,000 times, with a random interval between presentations. As a first approximation it was assumed that the stimulus and the oscillation elicited independent precise spike patterns. **a** | The response of the neuron aligned with the stimulus onset. **b** | The response aligned with the oscillation cycle, where the x ordinate for each spike is its phase with respect to the oscillation. The top panel contains a rastergram across the first 50 stimulus presentations (the data in blue) and a rastergram across the first 50 oscillation cycles (the data in red). The bottom panel shows the corresponding spike-time histograms across all data, with the stimulus-related spikes in red and the oscillation-related spikes in blue. When they are aligned with the stimulus onset, the stimulus-induced spikes are precise and the oscillation-related spikes form a random background. When the data are aligned on the oscillation cycle the situation is reversed, with the stimulus-related spikes forming a random background. **c**,**d** | Under realistic circumstances, there will be interaction between the stimulus-related and the oscillation-related synaptic inputs. Two simple cases are illustrated using the stimulus-aligned spike-time histograms. **c** | The delta oscillation modulated the number of spikes that were elicited by the stimulus presentation, with the higher rates occurring at the beginning of the oscillation cycle. The precision (the width of the peaks) was not affected but the spike count across trials was much more variable. **d** | The delta oscillation shifted the times of the stimulus-elicited spikes depending on when they occurred in the oscillation cycle. This reduced the precision: the first two peaks seem to have merged. If stimulus-related information is to be coded in the precise spike times, the interaction illustrated in part **c** is innocuous but the one in part **d** is harmful.

was repeated with synapses on different branches, the sigmoidal behaviour was absent. Apparently, each dendritic branch integrates its input independently through a local nonlinearity. This suggests a two step process: first, synchrony decoding occurs in the dendritic branches, and then global integration with the inputs from other dendritic branches at the soma follows[90].

In CA1 pyramidal cells in the hippocampus, an additional faster nonlinearity is generated by the activation of sodium channels[91]. In a landmark study, two-photon uncaging of caged glutamate was used to apply a spatial pattern of synaptic activation in hippocampal slices. When a dendritic action potential (dAP) was generated at the apical trunk it quickly propagated to the soma and elicited a reliable and precise action potential[91]. When the dAP was initiated in the oblique dendrites it propagated to the soma but did not lead to an action potential[92]. Instead, a rapid voltage deflection was observed at the soma, followed by a slower (but still nonlinear) deflection that was due to calcium entry. In order to generate a dAP, the synaptic inputs to the cell needed to be both spatially clustered (within 20 µm) and temporally coherent, occurring within a few milliseconds of each other (FIG. 7c,d). Spatiotemporally coherent input at the apical trunk was also more efficient at eliciting somatic action potentials.

These studies show that there are multiple ways to generate action potentials. Some methods lead to precise spikes that are conducive to generating synchronous volleys, whereas others are more appropriate for the propagation of firing rate modulations.

Gated temporal information transfer between cortical layer 4 and layer 2/3. Even though coherent synaptic activation makes feedforward propagation of spike volleys possible, inhibitory circuits and recurrent loops could gate the propagation of spike volleys and influence their timing. Consider, for example, the feedforward pathway in the visual cortex that originates from thalamocortical relay cells that project to layer 4 spiny stellate cells (SSCs), which in turn project to layer 2/3 pyramidal cells[93] (FIG. 7a). Thalamocortical synapses are more effective than intracortical synapses[94], but they form only a small fraction of the synapses onto SSCs[95,96].

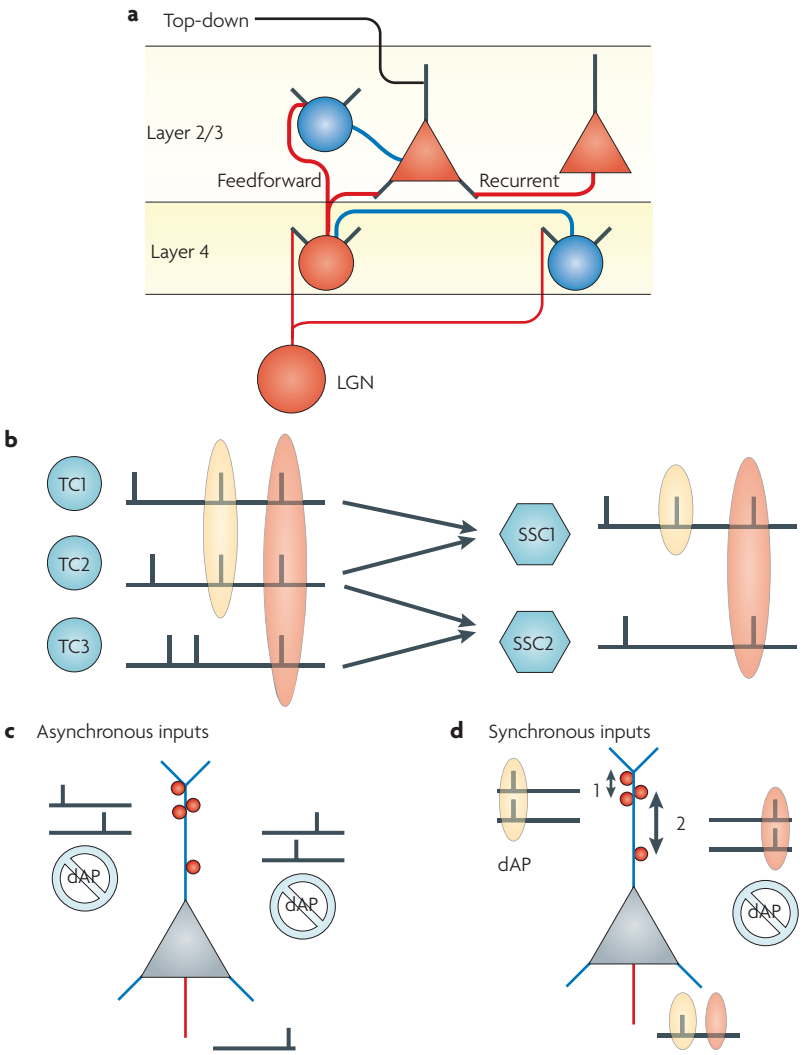

Figure 7 | **Experimental observations suggest that volleys that are generated by spike patterns are preferentially processed in the early sensory cortex. a** | A simplified representation of the laminar structure of the feedforward pathway in cortical area V1. Thalamocortical (TC) cells project to spiny stellate cells (SSCs) in layer 4, which in turn project to layer 2/3 pyramidal cells. The layer 2/3 pyramidal cells receive feedforward input from layer 4, recurrent inputs from other pyramidal cells and top-down inputs from other cortical areas (such as V2). In both layer 4 and layer 2/3 there is feedforward inhibitory input. The inhibitory cells and their projections are shown in blue, whereas the excitatory cells and their projections are shown in red. **b** | TC cells project to SCCs in layer 4 of the sensory cortex. Experimental recordings of TC neurons indicate the presence of spike patterns[18,43], which suggests that there are synchronous spike volleys at the population level. The spike volleys could be synchronous to a few SSCs (yellow highlight) or they could be synchronous across inputs to a large group of SSCs (red highlight). Synapses made by TC cells are more effective than intracortical synapses, but there are fewer of them. Nevertheless, because of synchronous spikes the TC cells as a group are effective[98]. At the cortical level, this leads to synchronous output spikes across the SSC population when the synchrony extends across many TC cells (red highlight), but not when it is limited to only a few TC cells (yellow highlight). **c**,**d** | Pyramidal cells in layer 2/3 (REF. 140) and layer 5 (REF. 141) of the cortex, and those in hippocampus[91,92], display dendritic action potentials (dAPs) that move towards the soma where, in many cases, they lead to a precise and reliable output spike. Experiments in the hippocampus that used caged glutamate established the conditions under which dAP are generated[91]. **c** | dAP were not obtained when a pyramidal cell was stimulated by asynchronous spike trains. Target synapses are depicted as red circles. **d** | dAP were obtained when the input spike trains were synchronous and the synapses they activated were close together (clustered) on the dendrite (arrow 1; synaptic distance less than 20 µm); they were not obtained when the synapses were further apart (arrow 2; synaptic distance more than 20 µm). LGN, lateral geniculate nucleus.

Nevertheless, collectively they seem to be efficient in driving the SSCs[45,97]. The reason for this efficiency was elucidated in another cortical area, in neurons that project from the ventroposteromedial thalamus (VPM) to the barrel cortex[98] and that respond to whisker movement. Membrane deflection in a SSC in response to a single spike in a presynaptic thalamocortical neuron was small compared to the depolarization that was caused by sensory events. Nevertheless, because rapid whisker deflections caused synchronous thalamocortical spikes, the SSC spiked reliably (FIG. 7b). The authors estimated that approximately 30 of the 85 thalamocortical cells that projected to a given cell were simultaneously active[98]. Simulations of the impact of synchronous thalamic inputs to a detailed compartmental model of a reconstructed SSC confirmed the experimental findings and further revealed the importance of having balanced background inputs from other cortical cells[99]. The experimentally observed spike patterns in the lateral geniculate nucleus correspond at the population level to synchronous volleys. Taken together with experimental results from other sensory modalities[48,100], this suggests that the output of SSCs might also consist of spike volleys.

In the cat primary visual cortex, the response of thalamocortical cells to a briefly flashed square was compared to the response of layer 4 and layer 2/3 cortical cells[101]. The layer 4 response was reliable, but the layer 2/3 response was less reliable. Evidence for the role of inhibition in synaptic transmission from layer 4 to layer 2/3 is found in slice experiments in the rodent barrel cortex[102–105]. Taken together, these experiments point to the presence of a gating mechanism between layer 4 and layer 2/3, under the control of inhibition, that allows some signals but not others to propagate. At present, only the excitatory pathway has been studied in biophysically constrained models[106]. The laminar structure of the cortex[93,107], in which various recurrent loops are present, might have advantages for processing and transmitting sensory information in the form of spike times — as suggested in a recent modelling study[108].

Inhibition can modulate firing rate and influence spike times. Precise inhibition generated by fast cortical oscillations can gate and modulate the propagation of spike volleys. Cortical basket cells make synapses close to or directly onto the soma of pyramidal cells. In the hippocampus, the spike of one basket cell can synchronize the activity of a large number of pyramidal cells[109]. Inhibitory cells are involved in the generation of fast oscillations, especially those in the gamma frequency range[110,111]. Consistent with this role, for *in vivo* recordings the power spectrum of currents generated by inhibitory synapses has more power in the gamma frequency range than the power spectrum of currents generated by excitatory synapses[112]. To test the impact of inhibitory currents on neural spiking, currents representing inhibitory and excitatory inputs were injected at the soma using the dynamic clamp technique[112]. The properties of the injected current were adjusted so that the overall response properties of the neurons *in vitro* were the same as those of similar neurons *in vivo*. First the

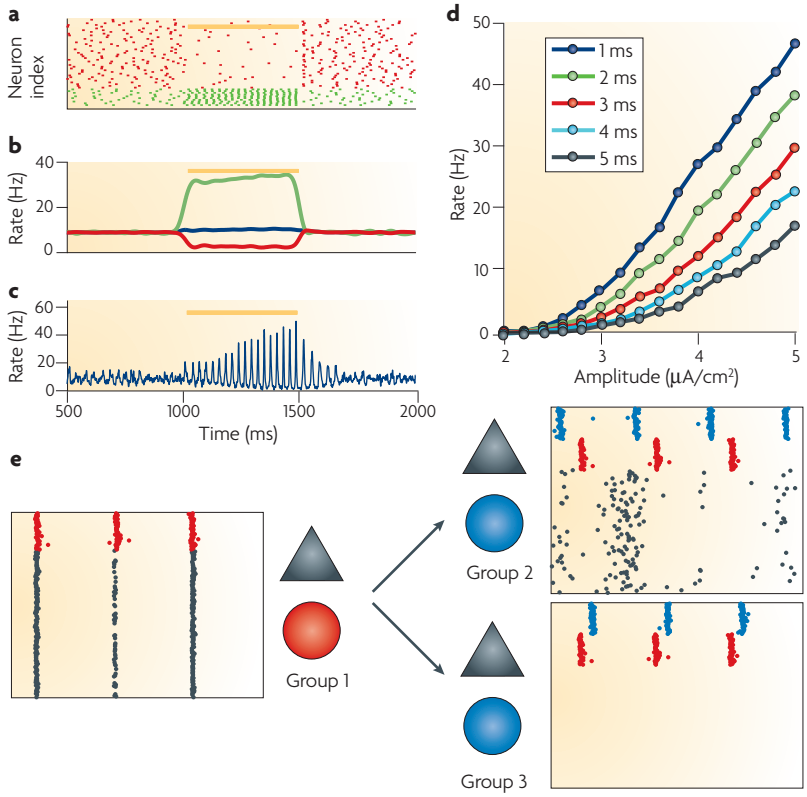

Figure 8 | **Attentional modulation of synchrony and phase in a model network. a–c** | Synchrony by competition. A network model with Hodgkin–Huxley-type neurons was used for the simulations[115]. **a** | In an inhibitory network of 1,000 neurons, 250 neurons (represented by the green dots) are transiently activated by a 500-ms depolarizing current pulse (represented by the yellow bar). The remaining 750 neurons (represented by the red dots) are not stimulated. The current pulse represents the effect of a top-down excitatory projection that has been hypothesized to mediate the effects of selective attention. **b** | The firing rate of the activated neurons increases (green line) but the mean stays approximately constant (blue line) because the non-activated neurons are suppressed (red line). **c** | The network as a whole synchronizes, as indicated by the sharper and higher peaks in the graph. **d** | The transformation of synaptic inputs into an output spike train is often characterized quantitatively as the firing rate (f) that is obtained in response to the injection of a current step as a function of the amplitude (I) of the step (the f–I characteristic). A gain change of the f–I means that, for the same value of I, a different firing rate is obtained (expressed as a gain factor (g) times the old firing rate (f)). The gain change is multiplicative when g is independent of the value of I. Changes in the synchrony (precision) of inhibitory inputs, such as those that are generated in the interneuron network in **a**, change the gain of postsynaptic neurons in an approximately multiplicative way. Decreasing jitter increases the firing rate. The value of the jitter for each curve, expressed in milliseconds, is shown in the key. The data were obtained from simulations of a single-compartment model[116]. **e** | An example of selective communication using phase relationships. There were 3 pools of neurons, each comprising 200 pyramidal cells (represented by the black triangles) and 50 interneurons (represented by the blue and red circles). The group 1 neurons projected to the group 2 and 3 neurons. The rastergrams are colour-coded according to the colour of the symbol for each cell group. The interneurons in each group were synchronized but had different phases. Group 1 interneurons (represented by the red dots) lagged behind those in group 2 (represented by the blue dots in the right-hand upper panel) but led those in group 3 (represented by the blue dots in the right-hand lower panel). As a result, when an excitatory volley from group 1 (represented by the black dots in the left-hand panel) arrived in group 2, the inhibition had already partially decayed and the neurons responded (represented by the black dots in the right-hand upper panel). Conversely, for group 3 the excitatory volley arrived at the time with the highest inhibition, and no spikes were produced. The spikes of the interneuron network in group 1 (red dots) are repeated in the rastergrams for groups 2 and 3 to provide a reference time. Simulation data were obtained from a network model similar to one used previously to study attentional modulation in cortical area V4[118]. Parts **a** and **c** reproduced, with permission, from REF. 115 © (2004) MIT Press. Part **d** reproduced, with permission, from REF. 116 © (2004) Elsevier Science.

same segment of the inhibitory conductance waveform was injected multiple times, each time with a different segment of the excitatory conductance waveform. Then the reliability and precision of the neuron's spike train was determined. Next the excitatory conductance segment was repeated and the inhibitory conductance was held constant. The repeated inhibitory conductance led to a higher precision than the repeated excitatory conductance. To find out what type of input most effectively drives the cell *in vivo*, a reverse correlation analysis[113] was performed on the inhibitory and excitatory conductance waveforms separately[114]. This showed that spikes of neurons in the association cortex of the cat were on average preceded by a reduction in inhibition. Neurons are, so to speak, driven by disinhibition.

In network models[115], interneurons can be transiently synchronized through 'synchrony by competition' (FIG. 8a–c), in which a top-down projection depolarizes a subset of interneurons, increasing their firing rate and synchrony. This reduces the firing rate of the remaining interneurons and synchronizes the 'winners'. Recent modelling work advanced the hypothesis that the effects of selective attention are mediated by the top-down activation of interneurons[116–121]. Taken together, the different aspects of this model[115] predict that selective attention strongly increases the firing rate of a subset of inhibitory neurons; this was recently confirmed experimentally[122].

When an interneuron network is in a synchronized oscillation, a postsynaptic neuron will receive volleys of synchronized inhibitory inputs from the network. In the model, a change in interneuron synchrony could affect the postsynaptic neuron in two ways[116]. The first is by a process called multiplicative gain (FIG. 8d), which could mediate the changes in firing rate that are seen in conjunction with selective attention[123]. Multiplicative-gain modulation is important because it increases or decreases the overall strength of the neuron's response while preserving the stimulus preference of the neuron[124]. The timescale of the inhibitory conductance is such that this modulation is better achieved for oscillations in the gamma frequency range[116]. Second, changes in interneuron synchrony could act as a gate, preventing spiking when the network is asynchronous and allowing spiking when the network is synchronous. In either case, the neuron produces spikes that are precisely timed with respect to the inhibitory rhythm. In principle, information could be coded in the fraction of cycles in which a spike is produced — the firing rate — or in the relative phase at which a spike is produced[125,126]. If the phase of each spike advances with each cycle, as it does in the hippocampus[127], early spikes could evade feedforward inhibition and have a competitive advantage. In general, the timing of synaptic inputs relative to the postsynaptic spike in an oscillatory cell could increase or decrease its strengths by spike-time dependent synaptic plasticity.

Only excitatory inputs that arrive during the period when the inhibitory conductance is low can be transmitted into an output spike, which is locked to the local inhibitory rhythm. This allows for a form of selective communication[128,129] (FIG. 8e). Using this mechanism, the specific path that feedforward information

Basket cell
A type of interneuron that sends its axon to the cell body of the postsynaptic cell and surrounds it with a structure akin to a basket.

Dynamic clamp
A technique by which the effect of opening ionic channels (a conductance change) is simulated by injecting into a real neuron a current that is proportional to the neuron's membrane potential.

Network model
A model comprised of neurons connected by synapses that is used to study the effects of synaptic coupling on the dynamics of neural activity.

Selective attention
A cognitive process that is involved in selecting stimuli based on their behavioural relevance.

follows along multiple groups could be rapidly altered to achieve behavioural goals. A re-analysis of *in vivo* data showed that transient correlations between spike trains in different cortical areas in the cat and in the macaque occurred predominantly during 'good' phase relationships between the respective LFPs in the gamma frequency range[130]. Slower rhythms have an important role in this process not only because they set the excitability of the neurons involved, but also because they set the amplitude of the fast rhythms[63,131], which determines how strong the gating is.

According to the traditional view, cortical interneurons, through tonic inhibition, control the firing rates of pyramidal neurons — a type of static control. The experiments and models that we have summarized here indicate that inhibitory interneurons have a more dynamic role, one that might be of critical importance for regulating the flow of information in the cortex by controlling spike timing and synchrony in cortical circuits[132].

Conclusion

Overall, the spike trains that are produced by a cortical pyramidal cell depend on the coherent states that are generated by recurrent columnar connectivity, the activation of top-down projections, and the current sensory stimulation through the feedforward pathway. Each of these three types of input by itself can only modulate the pyramidal cell's output, which raises the question of the nature of the relationship between the temporal dynamics of the stimulus and the spike patterns that are generated by the pyramidal cell. In particular, what is the nature of the competition between stimulus locking and phase locking to internal rhythms? The research that we have reviewed here suggests that ensembles of neurons produce slowly modulated activity that is accompanied by coherent volleys, with fast rhythms (beta and gamma rhythms) perturbing the timing or even gating the transmission of volleys, and slower rhythms (alpha, theta and delta rhythms) controlling the amplitude of fast rhythms. Subcortical and top-down intercortical projections can influence information processing by modulating the phase of these rhythms. Data analysis methods can disentangle stimulus locking from phase locking and thus provide a means to investigate the role of spike timing.

To further explore and validate these suggestions one needs to be able to record simultaneously from ensembles in different cortical areas, identify the neuron type and be able to perturb spike times of individual neurons in order to probe the network dynamics. A particularly promising technology makes use of light-activated excitatory channels and inhibitory (Cl^-) pumps, obtained from archaebacteria, which have recently been sequenced and incorporated in neurons[14,15,133]. Inhibitory pumps expressed in motor neurons of *Caenorhabditis elegans* have been successfully activated *in vivo* by light pulses, resulting in a change in the animal's movement[15]. *In vitro*, a sequence of light pulses applied to a hippocampal pyramidal cell was used to shift the spike times produced by injection of a fluctuating current at the soma[14]. When performed *in vivo*, on multiple neurons simultaneously, this method can be used to synchronize the spike times of an ensemble of neurons at one location and determine the effect on other cortical areas or even perception.

Taken together, techniques to probe single-neuron dynamics[91], to determine anatomical connections[134] and to record and perturb ensemble dynamics[14,15], as well as new methods to analyse spike trains, are contributing to a better understanding of the dynamic nature of brain function. In the next decade, models and experiments will merge in a way that will allow rapid progress towards understanding the principles of neural computation.

1. Mainen, Z. & Sejnowski, T. Reliability of spike timing in neocortical neurons. *Science* **268**, 1503–1506 (1995).
2. Bryant, H. L. & Segundo, J. P. Spike initiation by transmembrane current: a white-noise analysis. *J. Physiol.* **260**, 279–314 (1976).
3. Reinagel, P. & Reid, R. Temporal coding of visual information in the thalamus. *J. Neurosci.* **20**, 5392–5400 (2000).
4. Liu, R. C., Tzonev, S., Rebrik, S. & Miller, K. D. Variability and information in a neural code of the cat lateral geniculate nucleus. *J. Neurophysiol.* **86**, 2789–2806 (2001).
5. Butts, D. A. *et al.* Temporal precision in the neural code and the timescales of natural vision. *Nature* **449**, 92–95 (2007).
6. Shadlen, M. & Newsome, W. The variable discharge of cortical neurons: implications for connectivity, computation, and information coding. *J. Neurosci.* **18**, 3870–3896 (1998).
7. Brenner, N., Strong, S. P., Koberle, R., Bialek, W. & de Ruyter van Steveninck, R. R. Synergy in a neural code. *Neural Comput.* **12**, 1531–1552 (2000).
8. Reyes, A. D. Synchrony-dependent propagation of firing rate in iteratively constructed networks *in vitro*. *Nature Neurosci.* **6**, 593–599 (2003).
9. de la Rocha, J., Doiron, B., Shea-Brown, E., Josic, K. & Reyes, A. Correlation between neural spike trains increases with firing rate. *Nature* **448**, 802–806 (2007).
10. Hessler, N. A., Shirke, A. M. & Malinow, R. The probability of transmitter release at a mammalian central synapse. *Nature* **366**, 569–572 (1993).
11. Zador, A. Impact of synaptic unreliability on the information transmitted by spiking neurons. *J. Neurophysiol.* **79**, 1219–1229 (1998).
12. Deuchars, J., West, D. C. & Thomson, A. M. Relationships between morphology and physiology of pyramid-pyramid single axon connections in rat neocortex *in vitro*. *J. Physiol.* **478**, 423–435 (1994).
13. Markram, H., Lubke, J., Frotscher, M., Roth, A. & Sakmann, B. Physiology and anatomy of synaptic connections between thick tufted pyramidal neurones in the developing rat neocortex. *J. Physiol.* **500**, 409–440 (1997).
14. Han, X. & Boyden, E. S. Multiple-color optical activation, silencing, and desynchronization of neural activity, with single-spike temporal resolution. *PLoS ONE* **2**, e299 (2007).
15. Zhang, F. *et al.* Multimodal fast optical interrogation of neural circuitry. *Nature* **446**, 633–639 (2007). **The authors of this paper inserted light-activated pumps in neurons and used light to modify the behaviour of *C. elegans*. This technique makes it possible to manipulate the activity of a large number of neurons at a high temporal resolution in order to test hypotheses regarding the function of synchronous and precise spike timing.**
16. Tiesinga, P. H. E., Fellous, J. M. & Sejnowski, T. J. Attractor reliability reveals deterministic structure in neuronal spike trains. *Neural Comput.* **14**, 1629–1650 (2002).
17. Tiesinga, P. H. E. Precision and reliability of periodically and quasiperiodically driven integrate-and-fire neurons. *Phys. Rev. E Stat. Nonlin. Soft Matter Phys.* **65**, e041913 (2002).
18. Fellous, J. M., Tiesinga, P. H. E., Thomas, P. J. & Sejnowski, T. J. Discovering spike patterns in neuronal responses. *J. Neurosci.* **24**, 2989–3001 (2004).
19. Hunter, J., Milton, J., Thomas, P. & Cowan, J. Resonance effect for neural spike time reliability. *J. Neurophysiol.* **80**, 1427–1438 (1998).
20. Cecchi, G. *et al.* Noise in neurons is message dependent. *Proc. Natl Acad. Sci. USA* **97**, 5557–5561 (2000).
21. Azouz, R. & Gray, C. M. Dynamic spike threshold reveals a mechanism for synaptic coincidence detection in cortical neurons *in vivo*. *Proc. Natl Acad. Sci. USA* **97**, 8110–8115 (2000).
22. Toups, J. V., Fellous, J.-M., Thomas, P. J., Tiesinga, P. H. & Sejnowski, T. J. Stability of *in vitro* spike patterns under variation of stimulus amplitude. *Abstr. - Soc. Neurosci.* 237.18 (2006).
23. Fellous, J. M. *et al.* Frequency dependence of spike timing reliability in cortical pyramidal cells and interneurons. *J. Neurophysiol.* **85**, 1782–1787 (2001).
24. Berry, M. & Meister, M. Refractoriness and neural precision. *J. Neurosci.* **18**, 2200–2211 (1998).
25. Berry, M., Warland, D. & Meister, M. The structure and precision of retinal spike trains. *Proc. Natl Acad. Sci. USA* **94**, 5411–5416 (1997).
26. Tiesinga, P. H. E. & Toups, J. V. The possible role of spike patterns in cortical information processing. *J. Comput. Neurosci.* **18**, 275–286 (2005).
27. Keat, J., Reinagel, P., Reid, R. C. & Meister, M. Predicting every spike: a model for the responses of visual neurons. *Neuron* **30**, 803–817 (2001).

28. Nowak, L. G., Sanchez-Vives, M. V. & McCormick, D. A. Influence of low and high frequency inputs on spike timing in visual cortical neurons. *Cereb. Cortex* **7**, 487–501 (1997).
29. Hutcheon, B. & Yarom, Y. Resonance, oscillation and the intrinsic frequency preferences of neurons. *Trends Neurosci.* **23**, 216–222 (2000).
30. Pike, F. G. *et al.* Distinct frequency preferences of different types of rat hippocampal neurones in response to oscillatory input currents. *J. Physiol.* **529**, 205–213 (2000).
31. Haas, J. S. & White, J. A. Frequency selectivity of layer II stellate cells in the medial entorhinal cortex. *J. Neurophysiol.* **88**, 2422–2429 (2002).
32. Schreiber, S., Fellous, J. M., Tiesinga, P. & Sejnowski, T. J. Influence of ionic conductances on spike timing reliability of cortical neurons for suprathreshold rhythmic inputs. *J. Neurophysiol.* **91**, 194–205 (2004).
33. Tiesinga, P. H. E., Fellous, J. M., Jose, J. V. & Sejnowski, T. J. Computational model of carbachol-induced delta, theta, and gamma oscillations in the hippocampus. *Hippocampus* **11**, 251–274 (2001).
34. White, J. A., Budde, T. & Kay, A. R. A bifurcation analysis of neuronal subthreshold oscillations. *Biophys. J.* **69**, 1203–1217 (1995).
35. Hunter, J. D. & Milton, J. G. Amplitude and frequency dependence of spike timing: implications for dynamic regulation. *J. Neurophysiol.* **90**, 387–394 (2003).
36. Beierholm, U., Nielsen, C. D., Ryge, J., Alstrom, P. & Kiehn, O. Characterization of reliability of spike timing in spinal interneurons during oscillating inputs. *J. Neurophysiol.* **86**, 1858–1868 (2001).
37. Liljenstrom, H. & Hasselmo, M. E. Cholinergic modulation of cortical oscillatory dynamics. *J. Neurophysiol.* **74**, 288–297 (1995).
38. Hasselmo, M. E. Neuromodulation and cortical function: modeling the physiological basis of behavior. *Behav. Brain Res.* **67**, 1–27 (1995).
39. Brody, C. D. & Hopfield, J. J. Simple networks for spike-timing-based computation, with application to olfactory processing. *Neuron* **37**, 843–852 (2003).
40. Pillow, J. W., Paninski, L., Uzzell, V. J., Simoncelli, E. P. & Chichilnisky, E. J. Prediction and decoding of retinal ganglion cell responses with a probabilistic spiking model. *J. Neurosci.* **25**, 11003–11013 (2005).
41. Uzzell, V. J. & Chichilnisky, E. J. Precision of spike trains in primate retinal ganglion cells. *J. Neurophysiol.* **92**, 780–789 (2004).
42. Meister, M. & Berry, M. J. The neural code of the retina. *Neuron* **22**, 435–450 (1999).
43. Reinagel, P. & Reid, R. C. Precise firing events are conserved across neurons. *J. Neurosci.* **22**, 6837–6841 (2002).
44. Koepsell, K. *et al.* in *COSYNE 2007 Meeting* (Salt Lake City, 2007).
45. Kara, P., Pezaris, J. S., Yurgenson, S. & Reid, R. C. The spatial receptive field of thalamic inputs to single cortical simple cells revealed by the interaction of visual and electrical stimulation. *Proc. Natl Acad. Sci. USA* **99**, 16261–16266 (2002).
46. Kumbhani, R. D., Nolt, M. J. & Palmer, L. A. Precision, reliability, and information-theoretic analysis of visual thalamocortical neurons. *J. Neurophysiol.* **98**, 2647–2663 (2007).
47. Buracas, G. T., Zador, A. M., DeWeese, M. R. & Albright, T. D. Efficient discrimination of temporal patterns by motion-sensitive neurons in primate visual cortex. *Neuron* **20**, 959–969 (1998).
48. Higley, M. J. & Contreras, D. Balanced excitation and inhibition determine spike timing during frequency adaptation. *J. Neurosci.* **26**, 448–457 (2006).
49. Wehr, M. & Zador, A. M. Balanced inhibition underlies tuning and sharpens spike timing in auditory cortex. *Nature* **426**, 442–446 (2003).
50. Bair, W. Spike timing in the mammalian visual system. *Curr. Opin. Neurobiol.* **9**, 447–453 (1999).
51. Albrecht, D. G., Geisler, W. S., Frazor, R. A. & Crane, A. M. Visual cortex neurons of monkeys and cats: temporal dynamics of the contrast response function. *J. Neurophysiol.* **88**, 888–913 (2002).
52. Gur, M., Beylin, A. & Snodderly, D. M. Response variability of neurons in primary visual cortex (V1) of alert monkeys. *J. Neurosci.* **17**, 2914–2920 (1997).
53. Kara, P., Reinagel, P. & Reid, R. C. Low response variability in simultaneously recorded retinal, thalamic, and cortical neurons. *Neuron* **27**, 635–646 (2000).
54. Buzsaki, G. Rhythms of the brain (Oxford Univ. Press, Oxford, 2006).
55. Raghavachari, S. *et al.* Gating of human theta oscillations by a working memory task. *J. Neurosci.* **21**, 3175–3183 (2001).
56. Bichot, N. P., Rossi, A. F. & Desimone, R. Parallel and serial neural mechanisms for visual search in macaque area V4. *Science* **308**, 529–534 (2005).
This paper provided support for the idea that feature-based attention is mediated by synchrony in the gamma frequency range.
57. Fries, P., Reynolds, J. H., Rorie, A. E. & Desimone, R. Modulation of oscillatory neuronal synchronization by selective visual attention. *Science* **291**, 1560–1563. (2001).
58. Radman, T., Su, Y., An, J. H., Parra, L. C. & Bikson, M. Spike timing amplifies the effect of electric fields on neurons: implications for endogenous field effects. *J. Neurosci.* **27**, 3030–3036 (2007).
59. Lin, S. C., Gervasoni, D. & Nicolelis, M. A. Fast modulation of prefrontal cortex activity by basal forebrain noncholinergic neuronal ensembles. *J. Neurophysiol.* **96**, 3209–3219 (2006).
60. Rodriguez, R., Kallenbach, U., Singer, W. & Munk, M. H. Short- and long-term effects of cholinergic modulation on gamma oscillations and response synchronization in the visual cortex. *J. Neurosci.* **24**, 10369–10378 (2004).
61. Makeig, S. *et al.* Dynamic brain sources of visual evoked responses. *Science* **295**, 690–694 (2002).
62. Lakatos, P., Chen, C. M., O'Connell, M. N., Mills, A. & Schroeder, C. E. Neuronal oscillations and multisensory interaction in primary auditory cortex. *Neuron* **53**, 279–292 (2007).
63. Lakatos, P. *et al.* An oscillatory hierarchy controlling neuronal excitability and stimulus processing in the auditory cortex. *J. Neurophysiol.* **94**, 1904–1911 (2005).
64. Klausberger, T. *et al.* Brain-state- and cell-type-specific firing of hippocampal interneurons *in vivo*. *Nature* **421**, 844–848 (2003).
65. Tukker, J. J., Fuentealba, P., Hartwich, K., Somogyi, P. & Klausberger, T. Cell type-specific tuning of hippocampal interneuron firing during gamma oscillations *in vivo*. *J. Neurosci.* **27**, 8184–8189 (2007).
66. Buzsaki, G. Theta oscillations in the hippocampus. *Neuron* **33**, 325–340 (2002).
67. Csicsvari, J., Hirase, H., Czurko, A., Mamiya, A. & Buzsaki, G. Oscillatory coupling of hippocampal pyramidal cells and interneurons in the behaving rat. *J. Neurosci.* **19**, 274–287 (1999).
68. Lee, H., Simpson, G. V., Logothetis, N. K. & Rainer, G. Phase locking of single neuron activity to theta oscillations during working memory in monkey extrastriate visual cortex. *Neuron* **45**, 147–156 (2005).
This paper showed that phase locking in cortical area V4 during a working memory task can be more informative than the changes in the firing rate about the stimulus held in the memory.
69. Jacobs, J., Kahana, M. J., Ekstrom, A. D. & Fried, I. Brain oscillations control timing of single-neuron activity in humans. *J. Neurosci.* **27**, 3839–3844 (2007).
The authors of this paper presented evidence for widespread phase locking of neurons to rhythms in the delta, theta and gamma frequency ranges.
70. Siapas, A. G., Lubenov, E. V. & Wilson, M. A. Prefrontal phase locking to hippocampal theta oscillations. *Neuron* **46**, 141–151 (2005).
The authors of this paper showed that single units in the prefrontal cortex are locked to the LFP in the hippocampus, providing evidence for long-range communication by spike patterns.
71. Destexhe, A., Rudolph, M. & Pare, D. The high-conductance state of neocortical neurons *in vivo*. *Nature Rev. Neurosci.* **4**, 739-751 (2003).
72. Nir, Y. *et al.* Coupling between neuronal firing rate, gamma LFP, and BOLD fMRI is related to interneuronal correlations. *Curr. Biol.* **17**, 1275–1285 (2007).
73. Fellous, J. M. *et al.* Recovering stimulus-related precision in the context of background oscillations with random trial-to-trial phase. *Abstr. - Soc. Neurosci.* 394.1 (2007).
74. Diesmann, M., Gewaltig, M. O. & Aertsen, A. Stable propagation of synchronous spiking in cortical neural networks. *Nature* **402**, 529–533 (1999).
75. Ikegaya, Y. *et al.* Synfire chains and cortical songs: temporal modules of cortical activity. *Science* **304**, 559–564 (2004).
76. Aviel, Y., Mehring, C., Abeles, M. & Horn, D. On embedding synfire chains in a balanced network. *Neural Comput.* **15**, 1321–1340 (2003).
77. Vogels, T. P. & Abbott, L. F. Signal propagation and logic gating in networks of integrate-and-fire neurons. *J. Neurosci.* **25**, 10786–10795 (2005).
78. Bi, G. Q. & Poo, M. M. Synaptic modifications in cultured hippocampal neurons: dependence on spike timing, synaptic strength, and postsynaptic cell type. *J. Neurosci.* **18**, 10464–10472 (1998).
79. Cossart, R., Aronov, D. & Yuste, R. Attractor dynamics of network UP states in the neocortex. *Nature* **423**, 283–288 (2003).
80. Mokeichev, A. *et al.* Stochastic emergence of repeating cortical motifs in spontaneous membrane potential fluctuations *in vivo*. *Neuron* **53**, 413–425 (2007).
81. Larkman, A. & Mason, A. Correlations between morphology and electrophysiology of pyramidal neurons in slices of rat visual-cortex.I. Establishment of cell classes. *J. Neurosci.* **10**, 1407–1414 (1990).
82. Stepanyants, A. & Chklovskii, D. B. Neurogeometry and potential synaptic connectivity. *Trends Neurosci.* **28**, 387–394 (2005).
83. Koch, C. *Biophysics of Computation* (Oxford Univ. Press, Oxford, 1999).
84. Stuart, G., Spruston, N. & Hausser, M. (eds) *Dendrites* (Oxford Univ. Press, Oxford, 1999).
85. Mel, B. W. Synaptic integration in an excitable dendritic tree. *J. Neurophysiol.* **70**, 1086–1101 (1993).
86. Migliore, M. & Shepherd, G. M. Emerging rules for the distributions of active dendritic conductances. *Nature Rev. Neurosci.* **3**, 362–370 (2002).
87. Magee, J. C. Dendritic integration of excitatory synaptic input. *Nature Rev. Neurosci.* **1**, 181–190 (2000).
88. Polsky, A., Mel, B. W. & Schiller, J. Computational subunits in thin dendrites of pyramidal cells. *Nature Neurosci.* **7**, 621–627 (2004).
89. Cash, S. & Yuste, R. Linear summation of excitatory inputs by CA1 pyramidal neurons. *Neuron* **22**, 383–394 (1999).
90. Poirazi, P., Brannon, T. & Mel, B. W. Pyramidal neuron as two-layer neural network. *Neuron* **37**, 989–999 (2003).
91. Gasparini, S. & Magee, J. C. State-dependent dendritic computation in hippocampal CA1 pyramidal neurons. *J. Neurosci.* **26**, 2088–2100 (2006).
In this study, two-photon scanning microscopy was used to apply realistic spatial patterns of synaptic inputs to CA1 pyramidal cells, allowing the authors to study synaptic integration. The authors showed that spatially clustered and temporally precise synaptic activation reliably elicits a precise action potential by activating a dendritic action potential.
92. Losonczy, A. & Magee, J. C. Integrative properties of radial oblique dendrites in hippocampal CA1 pyramidal neurons. *Neuron* **50**, 291–307 (2006).
93. Douglas, R. J. & Martin, K. A. Neuronal circuits of the neocortex. *Annu. Rev. Neurosci.* **27**, 419–451 (2004).
94. Gil, Z., Connors, B. W. & Amitai, Y. Efficacy of thalamocortical and intracortical synaptic connections: quanta, innervation, and reliability. *Neuron* **23**, 385–397 (1999).
95. Ahmed, B., Anderson, J. C., Douglas, R. J., Martin, K. A. & Nelson, J. C. Polyneuronal innervation of spiny stellate neurons in cat visual cortex. *J. Comp. Neurol.* **341**, 39–49 (1994).
96. Stratford, K. J., Tarczy-Hornoch, K., Martin, K. A., Bannister, N. J. & Jack, J. J. Excitatory synaptic inputs to spiny stellate cells in cat visual cortex. *Nature* **382**, 258–261 (1996).
97. Kara, P. & Reid, R. C. Efficacy of retinal spikes in driving cortical responses. *J. Neurosci.* **23**, 8547–8557 (2003).
98. Bruno, R. M. & Sakmann, B. Cortex is driven by weak but synchronously active thalamocortical synapses. *Science* **312**, 1622–1627 (2006).
The authors of this paper used an innovative technique to show that although the synapses from thalamocortical projection cells make up only a small fraction of the synapses on layer 4 SSCs, and have only an average unitary strength, they are effective in driving the cells because of their synchronous activation.
99. Berry, M. & Meister, M. Synchronous thalamic inputs drive cortical neurons reliably when excitatory and inhibitory inputs are balanced. *Abstr. - Soc. Neurosci.* 394.19 (2007).
100. DeWeese, M. R. & Zador, A. M. Non-Gaussian membrane potential dynamics imply sparse, synchronous activity in auditory cortex. *J. Neurosci.* **26**, 12206–12218 (2006).

101. Hirsch, J. A. *et al.* Synaptic physiology of the flow of information in the cat's visual cortex *in vivo*. *J. Physiol.* **540**, 335–350 (2002).
102. Wirth, C. & Luscher, H. R. Spatiotemporal evolution of excitation and inhibition in the rat barrel cortex investigated with multielectrode arrays. *J. Neurophysiol.* **91**, 1635–1647 (2004).
103. Beierlein, M., Fall, C. P., Rinzel, J. & Yuste, R. Thalamocortical bursts trigger recurrent activity in neocortical networks: layer 4 as a frequency-dependent gate. *J. Neurosci.* **22**, 9885–9894 (2002).
104. Petersen, C. C. & Sakmann, B. Functionally independent columns of rat somatosensory barrel cortex revealed with voltage-sensitive dye imaging. *J. Neurosci.* **21**, 8435–8446 (2001).
105. Lubke, J. & Feldmeyer, D. Excitatory signal flow and connectivity in a cortical column: focus on barrel cortex. *Brain Struct. Funct.* **212**, 3–17 (2007).
106. Sarid, L., Bruno, R., Sakmann, B., Segev, I. & Feldmeyer, D. Modeling a layer 4-to-layer 2/3 module of a single column in rat neocortex: interweaving *in vitro* and *in vivo* experimental observations. *Proc. Natl Acad. Sci. USA* **104**, 16353–16358 (2007).
107. Thomson, A. M. & Bannister, A. P. Interlaminar connections in the neocortex. *Cereb. Cortex* **13**, 5–14 (2003).
108. Haeusler, S. & Maass, W. A statistical analysis of information-processing properties of lamina-specific cortical microcircuit models. *Cereb. Cortex* **17**, 149–162 (2007).
109. Cobb, S., Buhl, E., Halasy, K., Paulsen, O. & Somogyi, P. Synchronization of neuronal activity in hippocampus by individual GABAergic interneurons. *Nature* **378**, 75–78 (1995).
110. Whittington, M. A., Traub, R. D. & Jefferys, J. G. Synchronized oscillations in interneuron networks driven by metabotropic glutamate receptor activation. *Nature* **373**, 612–615 (1995).
111. Fisahn, A., Pike, F., Buhl, E. & Paulsen, O. Cholinergic induction of network oscillations at 40 Hz in the hippocampus *in vitro*. *Nature* **394**, 186–189 (1998).
112. Hasenstaub, A. *et al.* Inhibitory postsynaptic potentials carry synchronized frequency information in active cortical networks. *Neuron* **47**, 423–435 (2005).
This paper showed that inhibitory conductance fluctuations have more power in the gamma frequency range than excitatory fluctuations, thus providing support for the role of inhibition in controlling the spike times.
113. Rieke, F., Warland, D., de Ruyter van Steveninck, R. R. & Bialek, W. *Spikes: Exploring the Neural Code* (MIT press, Cambridge, Massachusetts, 1997).
114. Rudolph, M., Pospischil, M., Timofeev, I. & Destexhe, A. Inhibition determines membrane potential dynamics and controls action potential generation in awake and sleeping cat cortex. *J. Neurosci.* **27**, 5280–5290 (2007).
115. Tiesinga, P. H. E. & Sejnowski, T. J. Rapid temporal modulation of synchrony by competition in cortical interneuron networks. *Neural Comput.* **16**, 251–275 (2004).
116. Tiesinga, P. H., Fellous, J. M., Salinas, E., Jose, J. V. & Sejnowski, T. J. Inhibitory synchrony as a mechanism for attentional gain modulation. *J. Physiol. (Paris)* **98**, 296–314 (2004).
117. Tiesinga, P. H. E. Stimulus competition by inhibitory interference. *Neural Comput.* **17**, 2421–2453 (2005).
118. Buia, C. & Tiesinga, P. Attentional modulation of firing rate and synchrony in a model cortical network. *J. Comput. Neurosci.* **20**, 247–264 (2006).
119. Mishra, J., Fellous, J. M. & Sejnowski, T. J. Selective attention through phase relationship of excitatory and inhibitory input synchrony in a model cortical neuron. *Neural Netw.* **19**, 1329–1346 (2006).
120. Niebur, E., Koch, C. & Rosin, C. An oscillation-based model for the neuronal basis of attention. *Vision Res.* **33**, 2789–2802 (1993).
121. Niebur, E. & Koch, C. A model for the neuronal implementation of selective visual attention based on temporal correlation among neurons. *J. Comput. Neurosci.* **1**, 141–158 (1994).
122. Mitchell, J. F., Sundberg, K. A. & Reynolds, J. H. Differential attention-dependent response modulation across cell classes in macaque visual area V4. *Neuron* **55**, 131–141 (2007).
The authors of this paper distinguished the spike trains of putative interneurons from those of putative excitatory neurons using the spike waveform. They found that, in absolute terms, interneurons are more strongly modulated by attention than excitatory cells.
123. McAdams, C. J. & Maunsell, J. H. Effects of attention on orientation-tuning functions of single neurons in macaque cortical area V4. *J. Neurosci.* **19**, 431–441 (1999).
124. Salinas, E. & Thier, P. Gain modulation: a major computational principle of the central nervous system. *Neuron* **27**, 15–21 (2001).
125. Hopfield, J. J. Pattern recognition computation using action potential timing for stimulus representation. *Nature* **376**, 33–36 (1995).
126. Tiesinga, P. H. E., Fellous, J. M., Jose, J. V. & Sejnowski, T. J. Information transfer in entrained cortical neurons. *Network* **13**, 41–66 (2002).
127. O'Keefe, J. & Recce, M. L. Phase relationship between hippocampal place units and the EEG theta rhythm. *Hippocampus* **3**, 317–330 (1993).
128. Fries, P. A mechanism for cognitive dynamics: neuronal communication through neuronal coherence. *Trends Cogn. Sci.* **9**, 474–480 (2005).
129. Fries, P., Nikolic, D. & Singer, W. The gamma cycle. *Trends Neurosci.* **30**, 309–316 (2007).
130. Womelsdorf, T. *et al.* Modulation of neuronal interactions through neuronal synchronization. *Science* **316**, 1609–1612 (2007).
Local cortical networks project to a large number of other local networks. The authors of this study observed that communication seems to be selective, because each local network has a different phase of gamma oscillation and only pairs of networks with a good phase relationship can exchange information.
131. Canolty, R. T. *et al.* High gamma power is phase-locked to theta oscillations in human neocortex. *Science* **313**, 1626–1628 (2006).
This study reported the existence of spatially-specific and task-dependent correlations between the amplitude of high-gamma rhythms and the phase of theta oscillations.
132. Salinas, E. & Sejnowski, T. J. Correlated neuronal activity and the flow of neural information. *Nature Rev. Neurosci.* **2**, 539–550 (2001).
133. Lima-Mainen, S., Hromadka, T., Zhang, F., Deisseroth, K. & Zador, A. M. Identifying neurons with Channelrhodopsin-2 during *in vivo* electrophysiology in rodents. *Abstr. - Soc. Neurosci.* 99.3 (2007).
134. Wickersham, I. R. *et al.* Monosynaptic restriction of transsynaptic tracing from single, genetically targeted neurons. *Neuron* **53**, 639–647 (2007).
This study presented a new anatomical technique for finding all the neurons that project to a given neuron, thereby providing constraints on cortical circuits.
135. Schreiber, S., Fellous, J. M., Whitmer, D., Tiesinga, P. & Sejnowski, T. J. A new correlation-based measure of spike timing reliability. *Neurocomputing* **52–54**, 925–931 (2003).
136. Wiskott, L., Fellous, J. M., Kruger, N. & von der Malsburg, C. Face recognition by elastic bunch graph matching. *IEEE Trans. Pattern Anal. Mach. Intell.* **19**, 775–779 (1997).
137. Victor, J. D. & Purpura, K. P. Nature and precision of temporal coding in visual cortex: a metric-space analysis. *J. Neurophysiol.* **76**, 1310–1326 (1996).
138. van Rossum, M. C. A novel spike distance. *Neural Comput.* **13**, 751–763 (2001).
139. Bezdek, J. C. Pattern recognition with fuzzy objective function algorithms (Plenum, New York, 1981).
140. Larkum, M. E., Waters, J., Sakmann, B. & Helmchen, F. Dendritic spikes in apical dendrites of neocortical layer 2/3 pyramidal neurons. *J. Neurosci.* **27**, 8999–9008 (2007).
141. Larkum, M. E., Zhu, J. J. & Sakmann, B. Dendritic mechanisms underlying the coupling of the dendritic with the axonal action potential initiation zone of adult rat layer 5 pyramidal neurons. *J. Physiol.* **533**, 447–466 (2001).

Acknowledgements
We thank P. J. Thomas, S. Schreiber, D. Spencer, H. -P. Wang, J. V. Toups and J. V. José for their contributions to the research presented in this Review. This work was supported by the Human Frontier Science Program (P.T.), US National Institutes of Health grant R01 MH068481 (T.J.S. & P.T.) and the Howard Hughes Medical Institute (T.J.S.).

FURTHER INFORMATION
Paul Tiesinga's homepage: http://neuro.physics.unc.edu
Jean-Marc Fellous' homepage: http://www.u.arizona.edu/~fellous/
Terrence J. Sejnowski's homepage: http://www.cnl.salk.edu
ALL LINKS ARE ACTIVE IN THE ONLINE PDF